Molecular Dynamics in Poly(methylphenylsiloxane) As Studied by Dielectric Relaxation Spectroscopy and Quasielastic Light Scattering

D. Boese,* B. Momper, G. Meier, F. Kremer, J.-U. Hagenah, and E. W. Fischer

Max-Planck-Institut für Polymerforschung, Postfach 3148, 6500 Mainz, FRG.
Received November 15, 1988; Revised Manuscript Received March 6, 1989

ABSTRACT: Poly(methylphenylsiloxane) with a molecular weight of M_w = 28 500 Da (Da = daltons) (T_g = −26 °C) was studied. Experimentally, the quantities measured were the dielectric loss $\epsilon''(\omega)$ and the intensity autocorrelation function $G^{(2)}(t)$ by quasielastic light scattering in the melt close to the glass transition temperature. We have fit the $\epsilon''(\omega)$ data at each temperature with the Havriliak–Negami equation and from that computed the dipole–dipole reorientation correlation function. A fit of a stretched exponential (Kohlrausch–Williams–Watts form) to the correlation function is directly compared with the results from light scattering, which are usually given in this functional form. We find quantitative agreement between these two methods when comparing the time correlation functions. The agreement between both methods leads to the conclusion that the collective dynamics measured by light scattering, related to macroscopic mechanical properties of the material, and the molecular dynamics of reorienting dipoles are the same for polymeric melts of high inherent viscosity.

Introduction

The large group of siloxane polymers has served as model materials for highly flexible chain molecules.[1] Among them, especially poly(methylphenylsiloxane) (PMPS), which forms a clear, colorless, heat-resistent liquid, has promising properties:[2] The atactic polymer is purely amorphous and has a convenient glass transition temperature obtained by DSC of about T_g = −25 °C. Up to now a great variety of different physical methods have been applied to study the dynamics of relaxation processes: Kerr effect,[3] ultrasonic relaxation,[4] dielectric relaxation,[5-7] and light scattering such as depolarized Rayleigh spectroscopy,[8] Brillouin spectroscopy,[9,10] and quasielastic light scattering[11,12] (QLS) (also known as photon correlation spectroscopy). Whereas in ultrasonics and Brillouin one measures the propagation and damping of sound waves, depolarized light scattering is sensitive toward localized rotational dynamics and their coupling to the environment. The extension to even shorter times by interferometrically resolved Raman lines[13] measures the free rotation of the phenyl ring, which is in agreement with the line width from incoherent neutron scattering on the same material.[14]

On the low-frequency side of the spectrum, however, usually two methods have been established to study the dynamics of slowly relaxing density fluctuations: broadband dielectric relaxation (DR) and photon correlation spectroscopy (PCS). For a series of materials the dynamics have been studied by both methods mentioned above.[15] The motion under study here is classified as the α-motion or primary relaxation process because it is related to the glass transition of the polymer, which has a Williams–Landel–Ferry (WLF) temperature dependence.

Usually good agreement has been found between the activation parameters characterizing the temperature dependence of the dynamics. On the other hand, however, the absolute values of the relaxation times at a given temperature differ.[15] This difference has up to now not seriously been investigated. To compare the results of the two methods mentioned above, we propose a new method of data analysis.

Experimental Section

PMPS was prepared by an anionic ring-opening polymerization of 1,3,5-trimethyl-1,3,5-triphenylcyclotrisiloxane. The full procedure and sample characterization is described elsewhere.[16] The weight- and number-averaged molecular weights were determined by gel permeation chromatography (GPC) to be M_w = 28 500 Da and M_n = 27 300 Da (Da = dalton) (M_w/M_n = 1.04) using a silica gel column with THF as eluent. The universal calibration concept with polystyrene standards was used.[2] The glass transition temperature T_g was determined from DSC at a heating rate of 20 K/min to be T_g = −26 °C.

The dielectric measurements covered the frequency range from 10^{-1} to 10^9 Hz. Three different measurement systems were used: (1) A Solartron-Schlumberger frequency response analyzer FRA 1254, which was supplemented by using a high-impedance preamplifier of variable gain,[17] covered the frequency range from 10^{-4} to 6×10^4 Hz. (2) In the audiofrequency range of 10 to 10^7 Hz, a Hewlett-Packard impedance analyzer 4192A was used. For both parts the sample material was kept between two condenser plates (gold-plated stainless steel electrodes). (3) For the measurements between 10^6 and 10^9 Hz, a Hewlett-Packard impedance analyzer 4191A was employed, which is based on the principle of a reflectometer. Therefore a smaller condenser was needed to hold the sample and mounted as a part of the inner conductor. All three arrangements were placed in custom-made cryostats in which the sample was placed in a stream of temperature-controlled nitrogen gas, which allows temperature adjustment from 100 up to 500 K within ±0.02 K. For further details see ref 40.

The sample used for light scattering was directly filtered through a 0.45-μm Millipore Teflon filter in to a dust free $^1/_2$-in.-o.d. light scattering cell. We measured a low Landau–Placzek ratio of LPR = 5.4 at room temperature to assure the absence of dust. The measurements were performed with a Spectra-Physics 2020 argon ion laser operating at λ = 514.5 nm with a power of 400 mW. Intensity autocorrelation functions were measured in the range of 1 μs up to 1 s on a Brookhaven BI 2030 full autocorrelator in the multiple-τ version. To provide a greater time range of up to 6 decades, usually two runs with different basic sample times were spliced together. The polarizations of the incident beam and of the scattered light were both vertical to the scattering plane, so the geometry measured is the V_V geometry. All spectra were recorded at a fixed scattering angle of θ = 90°. The temperature was controlled by a Huber HS 80 closed-cycle cryostat with a temperature stability within ±0.2 K. Further details of the experimental procedure are described elsewhere.[2]

Theory

A. When dealing with dielectric relaxation, the frequency-dependent complex permittivity $\epsilon^*(\omega) \equiv \epsilon'(\omega) - i\epsilon''(\omega)$ is related to the dipole moment time correlation function $\phi(t)$ by a one-sided Fourier or pure imaginary Laplace transformation, which reads

$$\frac{\epsilon^*(\omega) - \epsilon_\infty}{\epsilon_0 - \epsilon_\infty} = \int_0^\infty \exp[-i\omega t]\left[-\frac{d\phi(t)}{dt}\right] dt \qquad (1)$$

0024-9297/89/2222-4416$01.50/0

where ϵ_0 and ϵ_∞ are the limiting low- and high-frequency permittivities, respectively. As shown by Williams[18] the total dipole moment time correlation function $\phi(t)$ is given by

$$\phi(t) = \sum_i^N \sum_j^N \langle \mu_i(0)\mu_j(t)\rangle / \sum_i^N \sum_j^N \langle \mu_i(0)\mu_j(0)\rangle$$

where $\mu_j(t)$ denotes the elementary dipole moment in the chain at time t.

Since $\epsilon'(\omega)$ and $\epsilon''(\omega)$ are related to each other via a Kramers–Kronig relation, the further evaluation concentrates only on $\epsilon''(\omega)$ to extract $\phi(t)$ from measured quantities. This is done by a half-sided cosine transformation:

$$\phi(t) = \frac{2}{\pi}\int_0^\infty \frac{\epsilon''(\omega)}{\epsilon_0 - \epsilon_\infty}\frac{\cos \omega t}{\omega}\,d\omega \qquad (2)$$

To describe the frequency dependence of $\epsilon''(\omega)$ (or in general for $\epsilon^*(\omega)$) analytically, the simplest case of dielectric relaxation involves the Debye function, which does not give a sufficient description of the relaxation behavior in polymeric melts. Quite often the empirical function derived by Cole and Davidson is used, but it also shows systematic deviations.[19] Recent studies have indicated[20] that the Havriliak–Negami (HN) equation, given by eq 3, describes the complex permittivity within experimental accuracy. The HN equation reads[21]

$$\epsilon^*(\omega) = \epsilon_\infty + \frac{\epsilon_0 - \epsilon_\infty}{(1 + (i\omega\tau)^\alpha)^\gamma} \qquad (3)$$

with $0 < \alpha, \gamma \leq 1$, where α is a parameter characterizing a symmetrical broadening of the distribution of relaxation times and γ characterizes an asymmetrical broadening. In order to calculate $\phi(t)$ from eq 2 from the functional form of eq 3, one has to evaluate eq 2 numerically after substituting the expressions for $\epsilon''(\omega)$ that read[20]

$$\epsilon''(\omega) = (\epsilon_0 - \epsilon_\infty) r^{-\gamma} \sin \gamma\psi \qquad (4)$$

$$r^2 = 1 + 2(\omega\tau)^\alpha \cos(\alpha\pi/2) + (\omega\tau)^{2\alpha} \qquad (5)$$

$$\tan\psi = \frac{(\omega\tau)^\alpha \sin(\alpha\pi/2)}{1 + (\omega\tau)^\alpha \cos(\alpha\pi/2)} \qquad (6)$$

The result of this numerical evaluation is a dipole–dipole autocorrelation function that can be compared with light scattering results usually given as time autocorrelation functions in a Kohlrausch–Williams–Watts (KWW) representation.

B. In a photon correlation spectroscopy experiment the measured quantity is the intensity autocorrelation function $G^{(2)}(t) \equiv \langle I(t)I(0)\rangle$ of the scattered light intensity I. For a Gaussian process in the homodyne case $G^{(2)}(t)$ is related to the autocorrelation function of the scattered field $g^{(1)}(t) \equiv \langle E(t)E(0)\rangle / \langle |E(0)|^2\rangle$ via

$$G^{(2)}(t) = \langle I\rangle^2(1 + f|g^{(1)}(1)|^2) \qquad (7)$$

where f is a constant. $g^{(1)}(t)$ is related to dynamic mechanical properties of the material when measuring in the VV geometry by[23]

$$\langle E(t)E(0)\rangle = a_1 G_{iso}(t) + a_2 G_{VH}(t) \qquad (8)$$

for a given $\mathbf{q}$ vector, where a_1, a_2 are constants and

$$G_{iso}(t) = [(\partial\epsilon/\partial\rho)_T]^2 \rho_0 N k_B T[D_e - D(t)] \qquad (9)$$

$$G_{VH}(t) = a_3^2 k_B T V[J_e - J(t)] \qquad (10)$$

Here a_3 is a constant, D is the longitudinal compressive compliance, J is the shear compliance, ϵ is the real part of the dielectric constant in the visible, ρ_3 is the average density, and N is the number of scatterers. It has been found experimentally that the time dependence of $G_{iso}(t)$ and $G_{VH}(t)$ is very similar,[24] so in all those cases where $I_{VH} \approx 0$, the use of eq 7 together with eq 8 provides us with the possibility of measuring directly the density autocorrelation function, which is proportional to the fluctuations of density given by

$$G_{iso}(t)_{\mathbf{q}} \equiv [(\delta\epsilon/\delta\rho)_T]^2 \langle \delta\rho(t)\delta\rho(0)\rangle_{\mathbf{q}} \qquad (11)$$

with $\mathbf{q}$ being the scattering vector. An experimental verification of eq 9 has been undertaken in the case of poly(vinyl acetate).[25] The mentioned comparison gives evidence that the findings from PCS as a method in the $\mathbf{q} \to 0$ limit yields results comparable with those from dynamic mechanical measurements.

Usually the shapes of density autocorrelation functions are highly asymmetric with respect to the log t scale. So far the best three-parameter fit to the measured data is given by the Kohlrausch–Williams–Watts (KWW) function

$$g^{(1)}(t) = a \exp[-(t/\tau_{KWW})^\beta] \qquad (12)$$

with $0 < \beta \leq 1$.[26] It is also possible to describe the experimental data by using the Laplace transformation of a distribution of retardation times $L(\ln\tau)$[26]

$$g^{(1)}(t) = \int_{-\infty}^{+\infty} \exp\left(-\frac{t}{\tau}\right) L(\ln\tau)\, d\ln\tau \qquad (13)$$

The distribution $L(\ln\tau)$ can be calculated from the experimental data by the complementary inverse Laplace transformation (ILT). From both representations mean relaxation times can be obtained via

$$\log\langle\tau\rangle = \frac{1}{2.303}\ln\left[\frac{\tau_{KWW}}{\beta}\Gamma\left(\frac{1}{\beta}\right)\right] \qquad (14)$$

where Γ denotes the Γ function or

$$\langle\log\tau\rangle = \frac{1}{2.303}\int_{-\infty}^{+\infty} (\ln\tau) L(\ln\tau)\, d\ln\tau \qquad (15)$$

The difference between the values from eq 14 and eq 15 for $0.4 < \beta < 1$ is less than 0.5 decades. A further discussion is given in the literature.[22,23]

Results and Discussion

The dielectric loss $\epsilon''(\omega)$ of PMPS has been measured for a number of different temperatures ranging from $T = -25.1$ °C up to $T = 55.3$ °C. From Figure 1a it is evident that in the cited range the maximum of loss shifts from $\log\nu = 0$ to almost $\log\nu = 8$. The experimentally accessible frequency range at the low-frequency end is limited by conductivity contributions and at high frequencies by resonance effects due to the sample geometry. In order to compare now the two sets of experiments ($\epsilon''(\omega)$ and $g^{(1)}(t)$ data), in principle two methods of calculation are possible. The obviously easiest way is to start with a KWW function, which is Fourier transformed and then directly compared with the measured $\epsilon''(\omega)$ data. This KWW function can also be used to compare directly with the light scattering result. But for the following reasons we decided not to do so. First, many data in the DR literature on glass-forming systems are adequately described by using the Havriliak–Negami function, so for reasons of continuity we decided to do the same, and second, we had in mind that it is very interesting to investigate the possible temperature dependence of the resulting HN parameters, especially while comparing them with the β KWW result. Therefore in order to apply eq

Table I
Havriliak–Negami Parameters $\Delta\epsilon_{HN}$, α, γ, and τ_{HN} and Kohlrausch–Williams–WaHs Parameters a, β, and τ_{KWW}[a]

T, °C	$\Delta\epsilon_{HN}$	α	γ	τ_{HN}, s	a	β	τ_{KWW}, s	$\langle\tau_{KWW}\rangle$, s
-22.8	0.42	0.76	0.56	4.7×10^{-2}	0.65	0.44	1.6×10^{-2}	4.2×10^{-2}
-21.1	0.41	0.80	0.46	1.7×10^{-2}	0.64	0.44	5.3×10^{-3}	1.4×10^{-2}
-19.1	0.40	0.82	0.43	5.1×10^{-3}	0.62	0.44	1.4×10^{-3}	3.7×10^{-3}
-17.0	0.40	0.84	0.39	1.7×10^{-3}	0.62	0.43	3.9×10^{-4}	1.1×10^{-3}
-11.2	0.35	0.76	0.56	7.6×10^{-5}	0.55	0.47	3.3×10^{-5}	3.4×10^{-5}
-9.7	0.35	0.77	0.55	4.1×10^{-5}	0.54	0.47	1.7×10^{-5}	3.8×10^{-5}
-7.8	0.34	0.83	0.46	2.3×10^{-5}	0.53	0.46	7.2×10^{-6}	1.7×10^{-5}
-6.0	0.34	0.85	0.43	1.3×10^{-5}	0.52	0.46	3.6×10^{-6}	8.5×10^{-6}
-4.0	0.34	0.89	0.36	7.1×10^{-6}	0.52	0.44	1.6×10^{-6}	4.2×10^{-6}
0	0.31	0.85	0.46	2.1×10^{-6}	0.48	0.47	6.7×10^{-7}	1.5×10^{-6}
23.4	0.25	0.96	0.34	1.7×10^{-8}	0.38	0.45	3.5×10^{-9}	8.7×10^{-9}
28.7	0.25	0.99	0.29	1.1×10^{-8}	0.38	0.43	1.8×10^{-9}	5.0×10^{-9}

[a] To describe the data within experimental accuracy (eq 3), variation of the fit parameters of $\Delta\epsilon_{HN} = \pm 0.005$, $\alpha = \pm 0.05$, $\gamma = \pm 0.06$, and $\tau_{HN} = \pm 10\%$ is possible. a, β, and τ_{KWW} parameters from the fit of $\phi(t)$ from eq 2 to the KWW representation of eq 12. $\langle\tau\rangle$ according to eq 14. The mean β value is $\bar{\beta} = 0.45 \pm 0.03$.

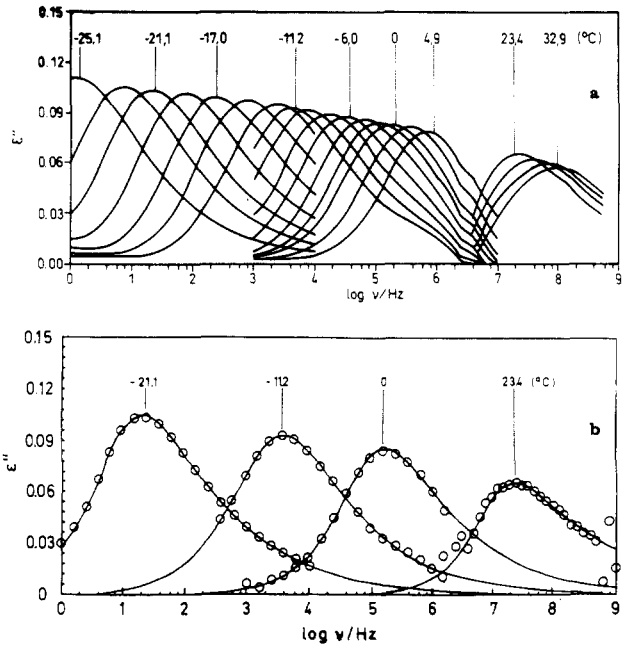

Figure 1. (a) $\epsilon''(\nu)$ versus log ν for PMPS (M_n = 28 500 Da with T_g = −26 °C) at different temperatures as indicated. At temperatures below T = −12.9 °C, the frequency response analyzer system was used; for very high frequencies, the reflectometer method was used. Accuracy of the measurement of the dielectric loss is ±5% in the low-frequency region; above 1 MHz the measurement accuracy is ±10%. (b) Data from (a) as fitted by using the Havriliak–Negami equation (3). The fit parameters are shown in Table I.

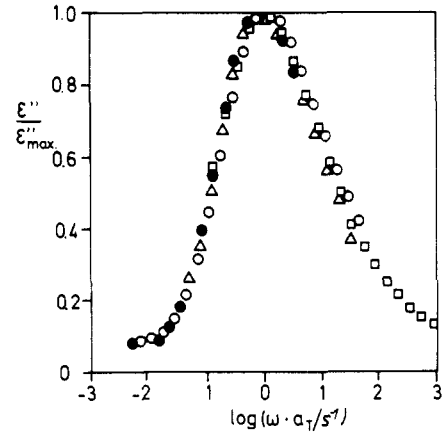

Figure 2. Master plot with T_{ref} = 0 °C. Plotted in normalized data $\epsilon''/\epsilon''_{max}$ from four different temperatures: (●) 0 °C; (△) −6 °C; (○) −17 °C; (□) −23 °C. The HN parameters of this curve are α = 0.80 and γ = 0.48. They are to compare with those from Table I.

2 to construct the $\phi(t)$ curve from the measured $\epsilon''(\omega)$ data, we have first fitted the data using the Havriliak–Negami approach according to eq 3 with respect to eq 4–6. The quality of the fit is demonstrated in Figure 1b. In Table I the results of the fit for selected temperatures almost covering the range given in Figure 1a are listed. From the analytical form of the ϵ'' data the $\phi(t)$ curves according to eq 2 were calculated by numerical integration. To the resulting correlation functions, the KWW function as given by eq 12 was fitted. The resulting β parameters are listed in Table I. The function was found to be remarkably constant over the entire temperature range.

This paper is not concerned with a physical model for the shape of the relaxation function. But for the discussion of several existing models,[28] it is important to notice that the β-KWW is constant but the HN α and γ show systematic temperature deviation. The coupling model of Ngai[29] predicts a crossover frequency of about 10^{10} Hz. With the highest frequency measured here (10^9 Hz), no change in the β-distribution parameter describing the ϵ'' data could be detected.

In a region $T_g + 10\text{ K} < T < T_g + 100\text{ K}$ the applicability of the WLF equation to describe the temperature dependence of the dynamic response of a system is generally accepted.[1] The equation reads

$$\log a_T = -\frac{C_1(T - T_0)}{C_2 + T - T_0} \tag{16}$$

Here a_T is a shift factor ($a_T = \omega/\omega_{ref}$). C_1, C_2, and T_0 are constants. The WLF constants C_1 and C_2 are usually given with respect to $T_0 = T_g$ as the reference temperature. The WLF equation is a mathematical formulation of the temperature–frequency superposition principle.

Consequently we have tried to construct a master plot[30-32] of arbitrarily chosen data from Figure 1a. We choose normalized data $\epsilon''/\epsilon''_{max}$ for the master plot given in Figure 2 and T_{ref} = 0 °C. The temperature range used is almost the same as the one we will use for light scattering later. As one can see from Figure 2, we are able to construct a fairly good masterplot with some deviations at the high-frequency side. This master plot simply reveals the fact that the β parameter is constant as can be seen from Table I and corresponds to the findings of the PCS experiment. We have fitted the Havriliak–Negami equation to the master plot and find α = 0.80 and γ = 0.48. A curve with the latter parameters has been inverted by means of eq 2 to the correlation function. The result is given in Figure 3 by the filled symbols. We have fitted a KWW function defined in eq 12 to this correlation function and

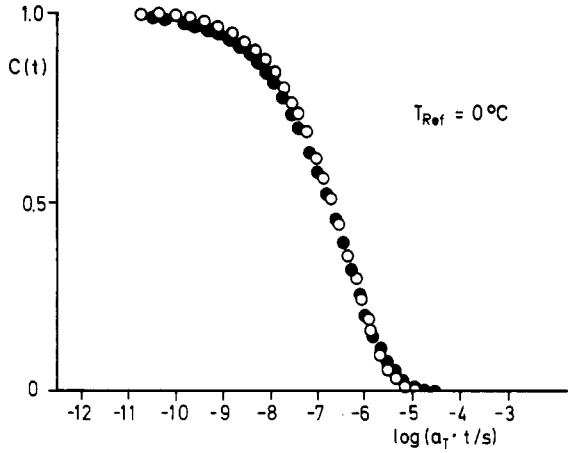

Figure 3. Normalized correlation function calculated according to eq 2 by using the HN parameter from Figure 2. The resulting β parameter (eq 12) is $\beta = 0.45$ (●). A correlation function with $\beta = 0.5$ (○), the distribution parameter from light scattering, is given for comparison for the same τ_{KWW}.

find for the β parameter a value of $\beta = 0.45$, which is identical with the mean β value given in Table I.

The concept of master curve (or the applicability of the time–temperature superposition principle) is also valid for the quasielastic light scattering experiment. In Figure 4a density autocorrelation functions of PMPS are shown measured in a temperature range from $T = -20$ °C up to $T = 5$ °C. In Figure 4b a master-curve construction for the same reference temperature $T = 0$ °C as for the DR data is given. We see that this construction is also nicely possible except for some deviations at the short time end. Since we have now introduced both master curves from either method, we compare the WLF constants derived from the temperature dependence of the shift factors. From PCS we get $C_1 = 14.8$ and $C_2 = 66.4$ K whereas from DR we extract $C_1 = 11.8$ and $C_2 = 67.9$ K. It is, however, a well-known fact that for the quite small accessible temperature range the determination especially of C_2 is uncertain. So precise data are only available from purely mechanical measurements in a temperature range of about $\Delta T \approx 100$ K.[1]

We therefore focus our attention on the determination of the dynamical response or the characteristic relaxation times. For that purpose we have to inspect the correlation functions from Figure 4 more closely. The attempt to fit eq 12 to the experimental data shows systematic deviations that are similar to the cases where primary and secondary relaxation processes are within the accessible time window of the PCS experiment.[33] In Figure 4c we have thus plotted the deviation from a best-fit single KWW function to the correlation function obtained at $T = -20$ °C to show that a single KWW representation is inadequate to fit the data. The usual approach to this kind of finding has been a double KWW function to account for the proper mathematical description of the data.[33] As this seems to be a very unphysical picture, we alternatively choose the inverse Laplace transformation (ILT) approach, first demonstrated for polymeric systems in the case of PMMA.[27] Consequently we have plotted in Figure 5 the ILT at two given temperatures to clearly demonstrate the double-bump feature of $g(t)$. The physical picture connected with this additional process, which is at a given temperature slower than the α relaxation, can be accounted for as a normal-mode process, equivalent to findings from ultrasonic relaxation[4,34] and dielectric relaxation.[35-38]

The assignment of the slow maximum in Figure 5 to a normal-mode process is indicated by two experimental

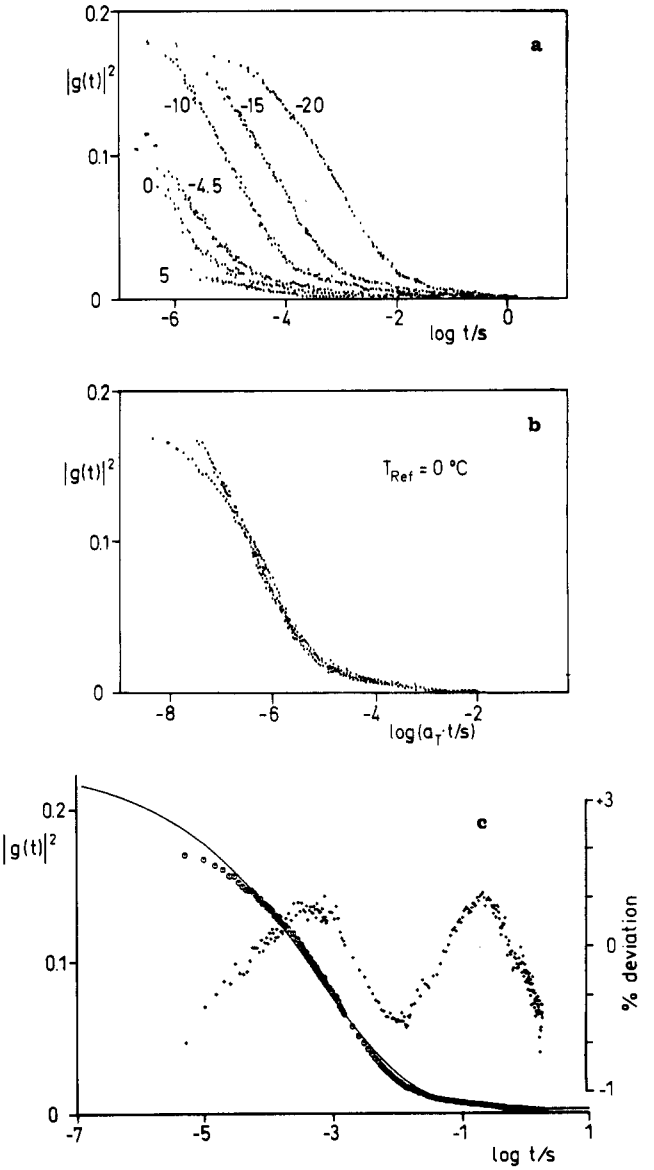

Figure 4. (a) Density autocorrelation functions of PMPS $|g^{(1)}(t)|^2$ versus log t measured at various temperatures given in the figure in degrees Celsius as indicated. Accuracy of the measurement is ±1%. (b) Master-curve construction of all the individually measured correlation functions shown in (a) with a reference temperature of $T_{ref} = 0$ °C. (c) The deviations in percent of a best-fit single KWW function (eq 12) to the correlation function of PMPS at $T = -20$ °C.

findings: First, by changing the molecular weights M of the samples under study, we find the mean times $\langle\tau\rangle$ varing with M^2 as it should according to the Rouse theory. Second, we find agreement between $\langle\tau\rangle$ from QLS and the prediction of $\langle\tau\rangle$ from steady-flow viscosity data on the same sample of known molecular weight.[39] This mode is not active in the DR experiment,[40] because the mean-square dipole moment in the polymer chain arises from the Si–O bond.[41,42] Due to the symmetry of the monomeric unit, the dipole moment components parallel to the main axis are not dielectrically active whereas they add up perpendicular to it. Consequently, in poly(*cis*-1,4-isoprene) a normal mode has been observed[35,36,40] with DR. The same holds for poly(propylene glycol) (PPG), where historically this effect has been observed for the first time.[38] This material is a good candidate to investigate the normal-mode process with DR and with QLS.

From the foregoing arguments it follows that the fast processes in Figure 5 are those to compare with the DR

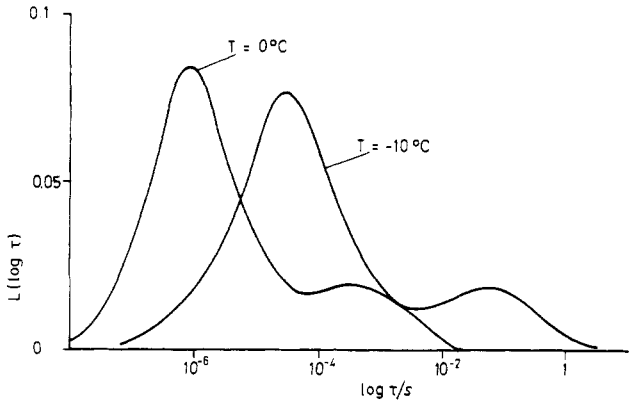

Figure 5. Results of the inverse Laplace transformation on two measured correlation functions of PMPS at $T = 0$ °C and $T = -10$ °C. From the figure the two-peak structure is evident in each case.

Table II
Fast Process of the $g(t)$ Data from Figure 4a in a KWW Representation According to Equation 12[a]

T, °C	τ_{KWW}, s	β	$\langle\tau_{KWW}\rangle$, s
−20	2.6×10^{-3}	0.52	4.8×10^{-3}
−15	1.7×10^{-4}	0.48	3.7×10^{-4}
−10	2.4×10^{-5}	0.48	5.2×10^{-5}
−4.5	4.0×10^{-6}	0.52	7.0×10^{-6}
0	8.0×10^{-7}	0.46	1.9×10^{-6}

[a] $\langle\tau\rangle$ according to eq 14. The mean β value in $\bar{\beta} = 0.50 \pm 0.03$.

results. To characterize the fast process in terms of mean time and distribution of times, one can either use the first moment of the distribution $L(\ln \tau)$, which gives $\langle \log \tau \rangle$ and the variance, which is a measure of the width of the distribution (the β parameter),[23] or use the approach of fitting a double KWW function to the data and compare only the fast part to DR.

In Table II the results of the fast portion of the double KWW fit to the data of Figure 4a are shown. To be sure, however, we have compared the results from both methods in terms of mean times and width of distribution and found them to be identical. The mean β-distribution parameter for die QLS data is 0.5 and so very close to the mean $\beta = 0.45$ from DR. To demonstrate the minor difference in the shape between $\beta = 0.45$ and $\beta = 0.5$ for the same τ_{KWW}, we have plotted in Figure 3 the latter correlation function with open symbols. From the temperature dependence of the $\langle\tau\rangle$ values given in Table II, we have extracted WLF parameters and find $C_1 = 14.8$ and $C_2 = 55.9$ K. The result now is in close agreement with the values from DR by less than 5% (estimated by using the Vogel–Fulcher–Tamman (VFT) form from which the activation parameter $B = 2.3C_1C_2$ can be calculated).

In Figure 6 we finally plot the logarithm of the mean time versus the reciprocal temperature. The points from DR are calculated by fitting eq 12 to the $\phi(t)$ data from eq 2. The times for QLS are from the fast part of the double KWW function, which gives the same result as the ILT analysis. Mean relaxation times are calculated in each case according to eq 14. As a result, we find the relaxation times of the process monitored with two different methods to be identical and further we note that also the shape parameters characterizing the relaxation time distribution are identical. This observation indicates that the responses obtained by two different methods are caused by one and the same relaxation process, although it is measured on a different length scale. Since the WLF behavior has its origin in long-time collective motions, it is indicated that

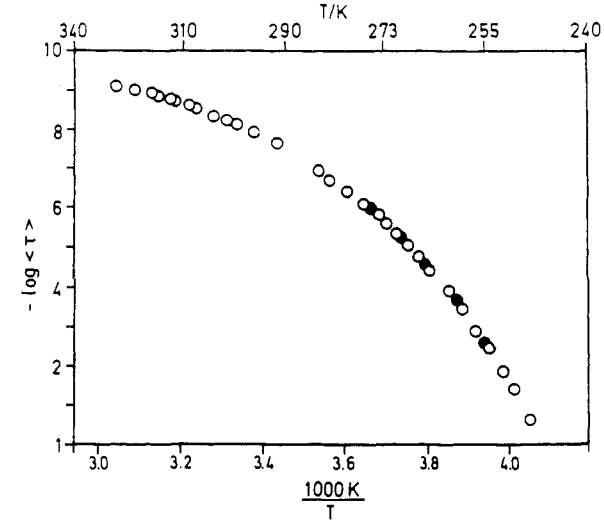

Figure 6. Plot of the logarithm of the mean relaxation times versus the reciprocal temperature. The open symbols (○) denote the DR data, the filled symbols (●), the QLS results.

the relevant relaxation times are the collective ones and govern the molecular dynamics. This is in quantitative agreement with the findings outlined in a recent publication by Ngai et al.[43]

Conclusions

The application of the Havriliak–Negami equation to the dielectric loss data $\epsilon''(\omega)$ provides an adequate functional form to calculate the dipole–dipole correlation function $\phi(t)$.

The distribution parameters α and γ of the Havriliak–Negami equation vary significantly with temperature, whereas the β parameter obtained from the Kohlrausch–Williams–Watts function remains constant.

It has been shown that the time correlation functions for both dielectric relaxation and photon correlation spectroscopy are found to be nearly identical.

For both methods the mean relaxation times were found to have the same temperature dependence and this leads to the conclusion that for poly(methylphenylsiloxane) the collective dynamics determine the molecular dynamics.

Acknowledgment. B.M. gratefully acknowledges the financial support of the Claussen-Stiftung im Stifterverband für die Deutsche Wissenschaft. G.M. acknowledges the financial support from the Sonderforschungsbereich 262.

Registry No. PMPS (homopolymer), 25569-20-4; PMPS (SRU), 9005-12-3.

References and Notes

(1) Ferry, J. D. *Viscoelastic Properties of Polymers*, 3rd ed.; J. Wiley: New York, 1980.
(2) Momper, B. Diploma Thesis, Mainz, 1986.
(3) Mendicuti, F.; Tarazona, M. P.; Saiz, E. *Polym. Bull.* **1985**, *13*, 263.
(4) Onabajo, A.; Dorfmüller, Th.; Fytas, G. *J. Polym. Sci., Polym. Phys. Ed.* **1987**, *22*, 749.
(5) Rushton, E.; Parry, J. V. L. *E. R. A. Tech. Rep. LIT* **1953**, 296.
(6) Dasgupta, S.; Smyth, C. P. *J. Chem. Phys.* **1967**, *47*, 2911.
(7) Baird, M. E.; Segupta, C. R. *J. Chem. Soc., Faraday Trans. 2* **1972**, *68*, 1795.
(8) Lin, Y. H.; Fytas, G.; Chu, B. *J. Chem. Phys.* **1981**, *75*, 2091.
(9) Wang, C. H.; Fytas, G.; Zhang, J. *J. Chem. Phys.* **1985**, *82*, 3405.
(10) Fytas, G.; Lin, Y. H.; Chu, B. *J. Chem. Phys.* **1981**, *74*, 3131.
(11) Fytas, G.; Dorfmüller, Th.; Lin, Y. H.; Chu, B. *Macromolecules* **1981**, *14*, 1088.
(12) Fytas, G.; Dorfmüller, Th.; Chu, B. *J. Polym. Sci., Polym. Phys. Ed.* **1984**, *22*, 1471.
(13) Samios, D.; Dorfmüller, Th. *Chem. Phys. Lett.* **1985**, *117*, 165.

(14) Meier, G.; Fujara, F.; Petry, W., unpublished results.
(15) See, e.g.: Fytas, G.; Patkowski, A.; Meier, G.; Dorfmüller, Th. *J. Chem. Phys.* **1984**, *80*, 2214.
(16) Momper, B.; Wagner, Th.; Ballauff, M., unpublished results.
(17) Pugh, J.; Ryan, J. T. *IEEE Conf. Dielectric Materials, Measurements Applications* **1979**, *177*, 404.
(18) Williams, G. *Chem. Soc. Rev.* **1977**, *7*, 89.
(19) Nozaki, S.; Mashimo, S. *J. Chem. Phys.* **1987**, *87*, 2271.
(20) Mashimo, S.; Nozaki, R.; Yagihara, S.; Taheishi, S. *J. Chem. Phys.* **1982**, *77*, 6259.
(21) Havriliak, S.; Negami, S. *Polymer* **1967**, *8*, 161.
(22) Hagenah, J.-U.; Meier, G.; Fytas, G.; Fischer, E. W. *Polym. J.* **1987**, *19*, 441.
(23) Hagenah, J.-U. Ph.D. Thesis, Mainz 1988.
(24) Fytas, G.; Wang, C. H.; Lilge, D.; Dorfmüller, Th. *J. Chem. Phys.* **1981**, *75*, 4247.
(25) Meier, G.; Hagenah, J.-U.; Wang, C. H.; Fytas, G.; Fischer, E. W. *Polymer* **1987**, *28*, 1640.
(26) Patterson, G. D. *Adv. Polym. Sci.* **1983**, *48*, 125.
(27) Fytas, G.; Wang, C. H.; Fischer, E. W.; Mehler, K. *J. Polym. Sci., Polym. Phys. Ed.* **1986**, *24*, 1859.
(28) Lindsey, C. P.; Patterson, G. D. *J. Chem. Phys.* **1980**, *73*, 3348.
(29) Ngai, K. L.; Fytas, G. *J. Polym. Sci., Polym. Phys. Ed.* **1986**, *24*, 1683.
(30) Williams, G.; Watts, D. C. *Trans. Faraday Soc.* **1970**, *66*, 80.
(31) Williams, G.; Watts, D. C.; Dev, S. B.; North, A. M. *Trans. Faraday Soc.* **1971**, *67*, 1323.
(32) Cook, M.; Watts, D. C.; Williams, G. *Trans. Faraday Soc.* **1970**, *66*, 2503.
(33) Meier, G.; Fytas, G.; Dorfmüller, Th. *Macromolecules* **1984**, *17*, 957.
(34) Alig, I.; Stieber, F.; Wartewig, S.; Fytas, G. *Polymer* **1988**, *29*, 975.
(35) Adachi, K.; Kotaka, T. *Macromolecules* **1984**, *17*, 120.
(36) Adachi, K.; Kotaka, T. *Macromolecules* **1985**, *18*, 466.
(37) Johari, G. P. *Polymer* **1986**, *27*, 866.
(38) Baur, M. E.; Stockmayer, W. H. *J. Chem. Phys.* **1965**, *43*, 4319.
(39) Momper, B.; Meier, G.; Fytas, G., unpublished results.
(40) Boese, D. Diploma Thesis, Mainz, 1987.
(41) Mark, J. E. *J. Chem. Phys.* **1968**, *49*, 1393.
(42) Mark, J. E.; Ko, J. H. *J. Polym. Sci., Polym. Phys. Ed.* **1975**, *13*, 2221.

Local Side Group Dynamics of Poly(methylphenylsiloxane) (PMPS) As Studied by Quasielastic Neutron Scattering

G. Meier,*,† F. Fujara,‡ and W. Petry§

Max Planck Institut für Polymerforschung, Postfach 3148, D-6500 Mainz, West Germany, Institut für Physikalische Chemie, Postfach 3108, D-6500 Mainz, West Germany, and Institut Laue Langevin, 156X, F-38042 Grenoble Cedex, France. *Received January 18, 1989; Revised Manuscript Received May 4, 1989*

ABSTRACT: Heterotactic PMPS has been used as a model system in order to study the occurrence of side group motion below and around the onset of the softening of the glassy structure. Incoherent quasielastic neutron scattering experiments and ^2H NMR spectra consistently identify this side group motion as a phenyl ring π-flip. The significance of this local motion process for the glass transition is discussed and put into the context of other available experimental results on the primary glass transition.

Introduction

The experimental and theoretical study of glass transitions is of high actual interest. Recent theoretical approaches[1] claim the occurrence of fast local dynamics (β-processes) as a precursor of the primary softening of the glassy structure (α-process) in *simple* liquids. The emphasis is on "simple"; i.e., β-processes are found in systems formed of Lennard-Jones particles without internal dynamics. So, a priori only interparticle dynamics is possible. Obviously the experimental verification of such β-processes depends on the availability of model systems resembling simple liquids as used in theory. However, *real* systems are much more complex. The more "simple" the liquid (metallic glasses etc.), the higher is its tendency to crystallize. In order not to leave the theoretical predictions only on the academic shelf, the experimentalist must allow for compromises and has to look for suitable real glass formers; but the search is not easy.

Networks (SiO_2, H-bridge types) certainly cannot be considered as good model systems because of the strong directional bondings, since it is expected that local dynamics is strongly coupled to structural degrees of freedom.

Molecular van der Waals liquids seem to be better model systems because of the individuality of their approximately spherical constituents. Intermolecular forces (van der Waals) are much weaker than intramolecular forces (bondings). Recently, it has been shown[2,3] that molecular liquids follow the predictions of mode coupling theory at least qualitatively. However, it is also true that in this case intramolecular motion cannot be fully excluded. The molecules are not necessarily stiff.

Polymers are also used to test theory. Although a chain represents an extended quasi one-dimensional bond structure, we again deal with intermolecular van der Waals bondings as in the case of molecular liquids. But of course, many more intramolecular modes may exist and interfere. Consequently polymers are by no means "simple". One way to avoid difficulties is to use main-chain polymers as is done in ref 4.

Let us adopt an opposite standpoint and look at a system where well-defined intramolecular motions, e.g., of side groups, are expected. Then we can ask again how such motions—to be called β-processes as well—are correlated with the glass transition. It was our goal to look for such a β-process. We chose a phenyl ring flip in a polymer. The system was chosen such that the phenyl ring flip is largely decoupled from other degrees of freedom and introduces a significant "dynamic" plasticizer effect; i.e., it triggers the glass transition.

We mainly performed incoherent quasielastic neutron scattering experiments because this method identifies the type of motion on a "microscopic" time scale which we believe to be the relevant time scale. The experiments are accompanied by some ^2H NMR spectra where the line shape is used for identifying the phenyl motion as a 180° rotational jump process.

† Max Planck Institut für Polymerforschung.
‡ Institut für Physikalische Chemie.
§ Institut Laue Langevin.

0024-9297/89/2222-4421$01.50/0